Disturbance cancellation in Compact Disc applications

Document Version:
Publisher's PDF, also known as Version of Record (includes final page, issue and volume numbers)

Please check the document version of this publication:

• A submitted manuscript is the version of the article upon submission and before peer-review. There can be important differences between the submitted version and the official published version of record. People interested in the research are advised to contact the author for the final version of the publication, or visit the DOI to the publisher's website.
• The final author version and the galley proof are versions of the publication after peer review.
• The final published version features the final layout of the paper including the volume, issue and page numbers.

[Link to publication](#)

Report of apprenticeship:

Disturbance cancellation in

Compact Disc Applications

By: M.J. v/d Molengraft

DCT 2001-61
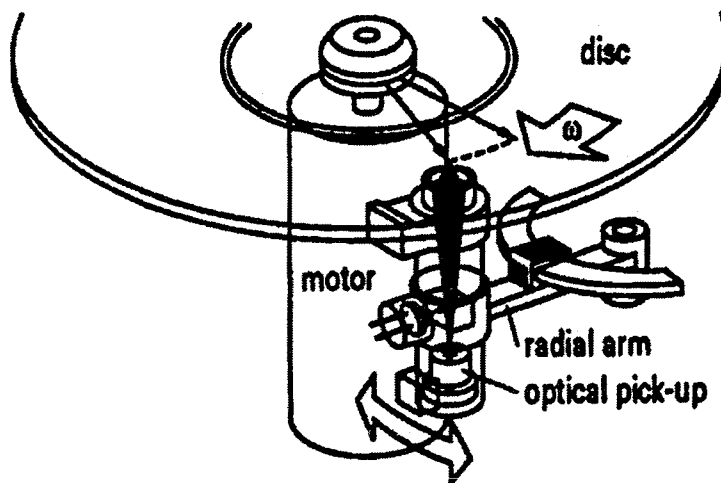
21 November 2001

Supervised by:
Prof. Dr. Ir. M. Steinbuch
Ir. P.W.J.M. Nuij

1 Introduction

The compact disc plays an important role in optical storage. At first the CD was mainly used in audio appliances. After some time the CD found its way to data storage in computer applications. For the audio appliances the demands on the controller are relatively low (accept for portable- and car stereo applications, where the player is submitted to shock loads). In the case of CD-ROM players the rotation frequency had to be increased to meet the wish of the consumer to get faster data access. With this increase in rotation frequency, the influence of periodic disturbances becomes larger, making the controller design harder.

A great deal of the periodic disturbance in the tracking error originates from the eccentricity of the track and the "wobbling" of the spindle motor during rotation. The tracking error has to stay within a tolerance limit for good performance. To reach this objective, the disturbances have to be counteracted.

In this paper, three different approaches to cancel the periodic disturbance, a notch-filter, an oscillator and a learning feedforward are presented and compared. In order to model the characteristics of the player, measurements on the sensitivity and the internal controller are done. The achieved model will be used in simulations of the three algorithms. After this, the methods will be implemented in a CDM9 player and the results will be compared.

In chapter 2 the algorithms are presented, chapter 3 contains the measurements and the modelling of the player, the simulations will be presented in chapter 4, results of implementation follow in chapter 5 and finally conclusions and recommendations will be given in chapter 6.

2 Disturbance canceling algorithms

To cancel the periodic disturbance, various algorithms are available. In this paper three approaches are discussed, a notch filter, an oscillator and a learning feedforward algorithm. Where the notch and the oscillator are rather straightforward, the LFF is more advanced. The main question is what improvement the LFF offers against standard techniques. To this extent the different algorithms are designed to have great similarity. The influence of the differences between the algorithms is investigated and evaluated.

The disturbance signal can be seen as a combination of sines and cosines at the rotational frequency and its harmonics. It can be modelled as follows:

$$d(t) = \sum_{i=1}^{n} \{a_i(t)\cos(\omega_i t) + b_i(t)\sin(\omega_i t)\}$$

(1)

Where $\omega_i = i * \omega_0$, with $f_0 = 2\pi * \omega_0$ being the rotational frequency. Manufacturing specifications for compact discs allow for a track eccentricity of 100 µm. Considering that the distance between the tracks on the CD is a mere 1.6 µm and the tracks are 0.4 µm wide (see figure 2.1), the maximum allowable error is specified to be 0.1 µm, meaning the sensitivity gain at the rotational frequency has to be less then –60 [dB] (a factor 1000).
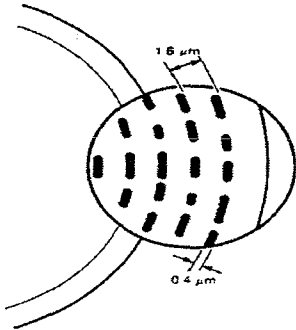

Figure 2.1: CD specifications

The overall system can be presented as below. Here the cancelling algorithm is a separate block (block A) **parallel** to a standard controller. The optical pickup in the CD-player returns the radial (track) error signal (RES), so the actual position of the laserspot is unknown. Since the desired value for the error is zero, a reference signal is omitted. The signal d represents the periodic disturbance (1).
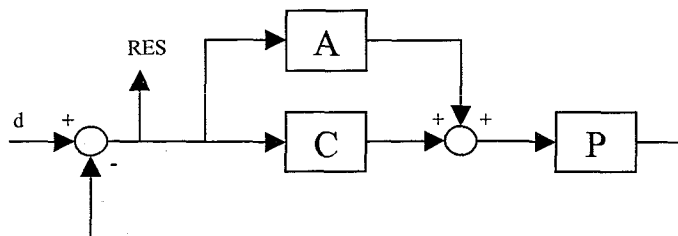

Figure 2.2: System

2.1 The notch filter

The notch filter is a standard control technique. In normal situations, the notch filter is used in series with the PID controller. Here the notch filter is used **parallel** to the PID. An inverted version of the notch filter is used; this results in a high controller gain, leading to a low sensitivity. In order to cancel the periodic

disturbance the notch filter is designed around the first harmonic of the rotational frequency, resulting in a low sensitivity at this frequency.

$$H_{notch} = \alpha \cdot \frac{s^2 + \beta_t \omega_t s + \omega_t^2}{s^2 + \beta_n \omega_n s + \omega_n^2} \qquad (2)$$

The parameters in the notch filter are designed to compensate for the sinusoidal error signal. The laplace transform of a sine and a cosine are respectively:

$$L[\sin(\omega t)] = \int \sin(\omega t) e^{-st} dt = \frac{\omega}{s^2 + \omega^2}$$

$$L[\cos(\omega t)] = \int \cos(\omega t) e^{-st} dt = \frac{s}{s^2 + \omega^2}$$

The main differences between these laplace transforms and the notch filter are the order of the numerator (s^2) and the damping in the denominator (β_n). Nothing can be done to lower the order of the numerator, but the damping in the denominator can be set to zero for more equivalence between filter and error signal. Both ω_t and ω_n are set at the rotational frequency ω_0.

2.2 The oscillator

Since the type of disturbance is known to be a combination of sinusoids, a so-called oscillation generator can be used to cancel it. The error can be cancelled by considering the nature of the error and adding a control signal of the same nature to the control signal generated by a conventional PID controller (the internal model principle).

$$H_{osc} = \alpha \cdot \frac{s + \omega}{s^2 + \omega^2} \qquad (3)$$

Here the differences between the error signal and the cancelling algorithm, as seen with the notch filter are gone, the order of the numerator is the same and there is no damping in the denominator. The oscillator does not differ much from the notch filter: the only difference is the order of the numerator.

2.3 The Learning Feedforward

As said before the learning feedforward is a more advanced algorithm. Again the nature of the error signal is taken into consideration. Due to the variation of actuator dynamics from player to player and the variation in eccentricity error from disc to disc the exact error signal is unknown. Thus an algorithm with constant parameters might not be adequate in all these situations. Therefore a learning feedforward is designed based on a least mean squares algorithm [1]. The algorithm presented in [1] is a discrete time version, in this paper a continuous version is used.

The error (1) can be cancelled with a control input of the following form:

$$u(t) = \hat{d}(t) = \sum_{i=1}^{n} \{\hat{a}_i(t)\cos(\omega_i t) + \hat{b}_i(t)\sin(\omega_i t)\}$$

The error will be exactly cancelled when the estimates of the coefficients have the true values:

$$\hat{a}_i(t) = a_i(t) \qquad \hat{b}_i(t) = b_i(t)$$

To achieve this a set of adaptive laws is designed to adjust the estimates:

$$\tfrac{d}{dt}\hat{a}_i(t) = \alpha_i y(t)\cos(\omega_i t + \phi_i)$$

$$\tfrac{d}{dt}\hat{b}_i(t) = \alpha_i y(t)\sin(\omega_i t + \phi_i)$$

The stability of the feedforward is analysed for the discrete time version in [1].

2.4 Parameter settings

The right settings for the parameters can be determined by using the sensitivity of the resulting closed loop (for the derivation of the model see chapter 3). However, since the learning feedforward is non-linear, neither closed loop function nor sensitivity is available.

Early simulations showed the same results for the oscillator and the learning feedforward with the same settings. This is confirmed in [2] where a lemma is stated and proved, saying that the learning feedforward scheme is equivalent to the internal model principle. See [2] for the proof. So if the settings for the oscillator are determined, they can be used for the feedforward as well. Figure 2.3 shows the sensitivities for the controller without an algorithm, for the controller with notch filter and for the controller with oscillator. The values for the parameters are set in such a way that the resulting system is stable (with sensitivity below 6 [dB] being the ideal situation). The value for α for the notch filter is set at .25 while the damping for the numerator β_n is set at .7 (β_d is set at 0.001). The value for α for the oscillator is set at 100. With these settings the maximum sensitivity is 6.87 for the notch and 6.56 [dB] for the oscillator, where the maximum is 5.08 for the controller without an algorithm. Figure 2.4 shows the relevant nyquist plots (keep in mind that the algorithms are placed **parallel** to the PID controller).
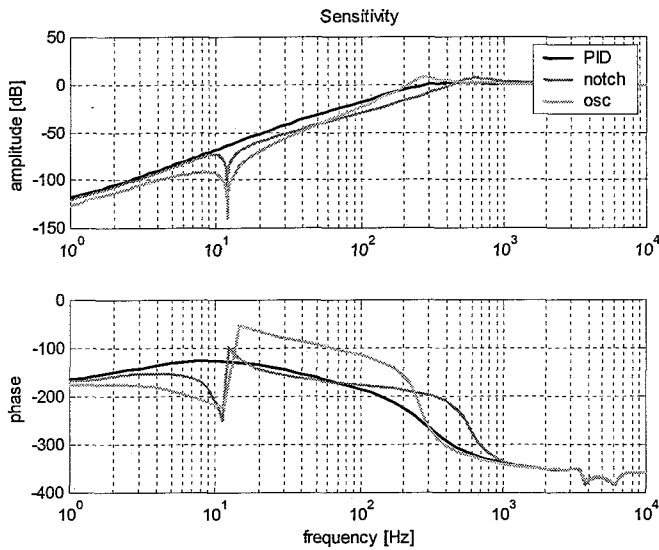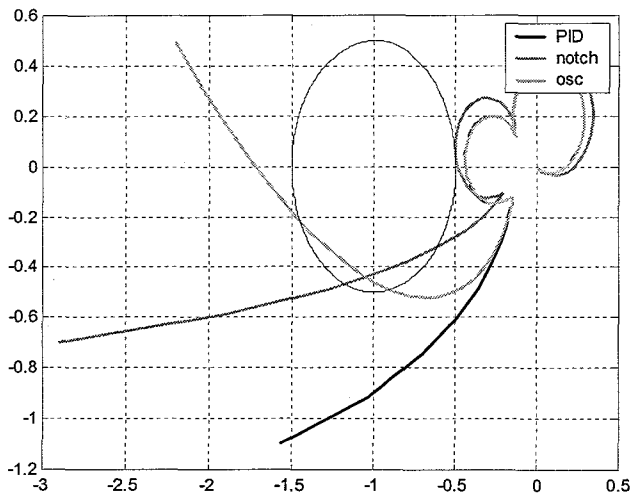

Figure 2.3: Sensitivity

Figure 2.4: Nyquist

3 Modelling the dynamics

For simulation purposes a model for the CD-player has to be determined. A way to determine the needed frequency response is by means of the sensitivity. When the sensitivity (S) and the controller (C) are known the plant (P) can be derived as follows.

$$S = \frac{1}{1+CP} \longrightarrow P = \frac{S^{-1}-1}{C} \tag{4}$$

The measurements are done using the virtual swept sine (VSS) option in the SigLab menu. The frequency range is split into two ranges, the first from 10 [Hz] to 500 [Hz] and the latter from 500 [Hz] to 10000 [Hz]. This is done so different accuracy levels can be set for these ranges (see appendix A). The same settings are used for all the measurements, to make calculations, such as extractions and multiplications, on the measurements easier. Figure 3.1 depicts the measurement setup.
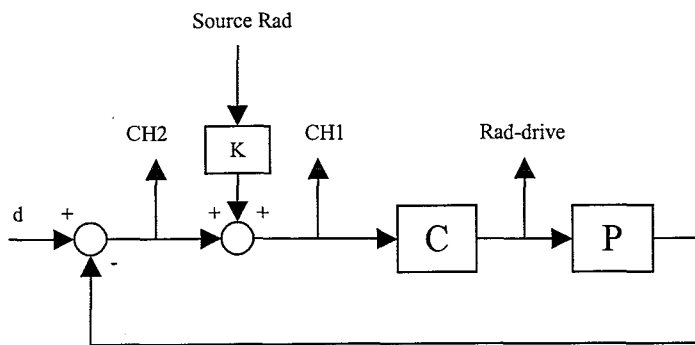

Figure 3.1: Measurement setup

3.1 Summation joint
The transfer of the summation joint may not be ideal. To see what the frequency response function is for this joint, the loop has to be opened. To open the loop the laser has to be turned off, this will lead to a feedback signal equal to zero, meaning no feedback, ergo no closed loop. When the loop is open, measuring the frequency response of the summation joint is achieved by measuring this response from "Source Rad" to CH1.
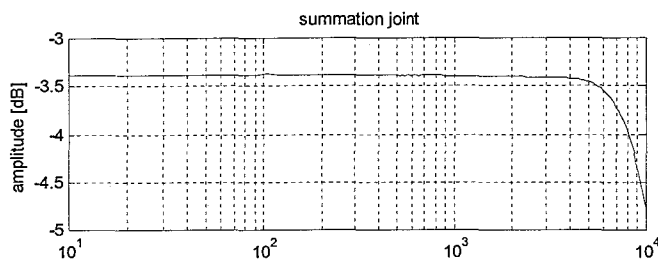

Figure 3.2: Frequency response summation joint

The summation joint appears to have a gain of –3.4 [dB] and a fall of after 5 [kHz]. The measurements on the controller and the sensitivity have to be corrected for this gain. Dividing the measurements with the frequency response for the joint will result in the correct data.

3.2 Sensitivity
The sensitivity can be measured around the summation joint. Again measuring the response from "Source Rad" to CH1, but now with the loop closed, will result in the wanted sensitivity. After correction for the summation joint the sensitivity is as follows.
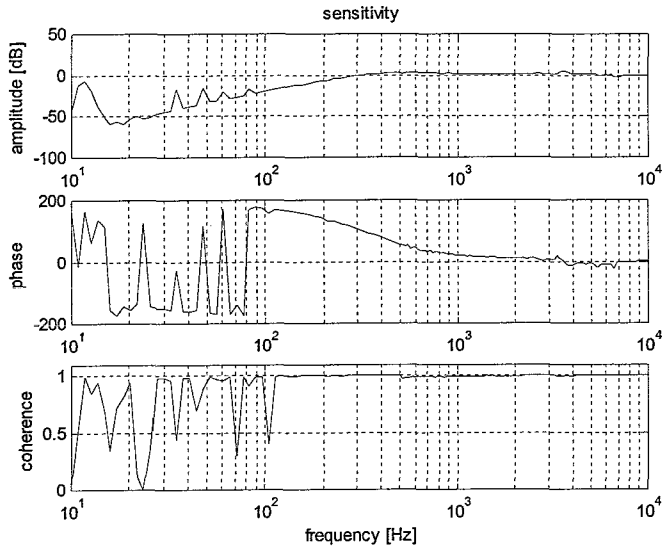
7

Figure 3.3: Sensitivity

The spikes at low frequencies are at the rotational frequency and its harmonics. At these frequencies the disturbance originating from the eccentricity dominates the error, resulting in a low signal/noise ratio. The coherence for these spikes was low so for the model they can be ignored.

3.3 Controller

In order to measure the controller, the loop has to be opened again. In the open loop situation measuring the response from "Source Rad" to "Rad-drive" results in the frequency response for the controller. Another way to derive the controller is an analytical one, using the electric charts for the print board [3]. In figure 3.4 the results are shown.
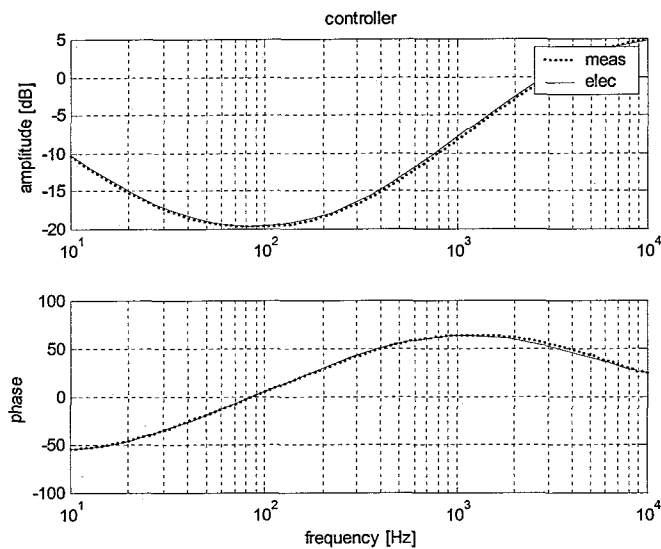

Figure 3.4: Frequency response controller

3.4 CD-player

Now using (4) the frequency response for the CD-player can be determined. In figure 3.5 this response is shown along with a 6th order fit. For this fit the routine "frfit" in MatLab is used. The spikes at the rotational frequency and its harmonics are ignored. The model will be used for the simulations in the next

8

chapter. Appendix B shows the resulting frequency response functions combined with the fitted model for measurements done on the CD-player for the following three cases: the inner track, the middle and the outer track of the disc. It is clear that the model is a good representation for the plant over the whole disc.
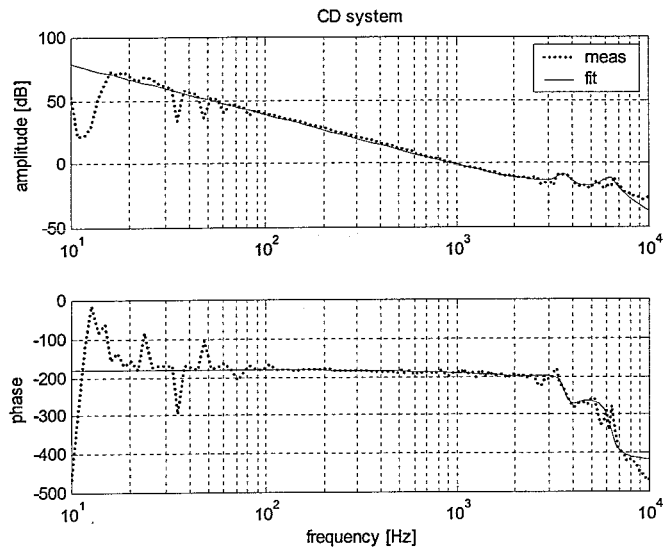

Figure 3.5: Frequency response CD-player

4 Simulation results

In the previous chapter a 6th order model was obtained. This model will now be used to simulate the performance of the three algorithms. In the simulations a measured error signal is used to obtain plausible results and to compare the resulting errors for the three algorithms with the measured one. To measure the error again a SigLab is used. In this case the option "virtual network analyzer" (VNA) is used. For the settings see appendix A. The radial disturbance can be obtained from the error signal by using the inverse sensitivity after filtering the low and high frequencies out of the error signal [3]. In figure 4.1 a measured error signal is shown along with its power spectrum calculated with the MatLab function "[power, frq] = psd(error, 2^9, f_s, hanning(2^9), 2^8)", f_s being the sample frequency. Figure 4.2 shows the obtained radial disturbance.
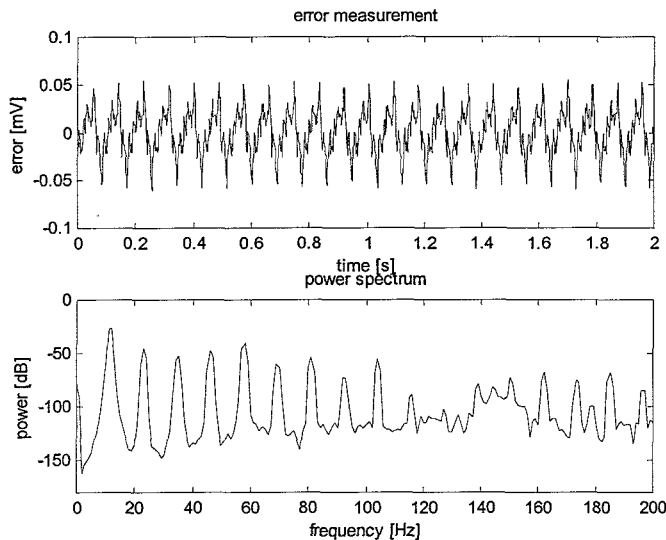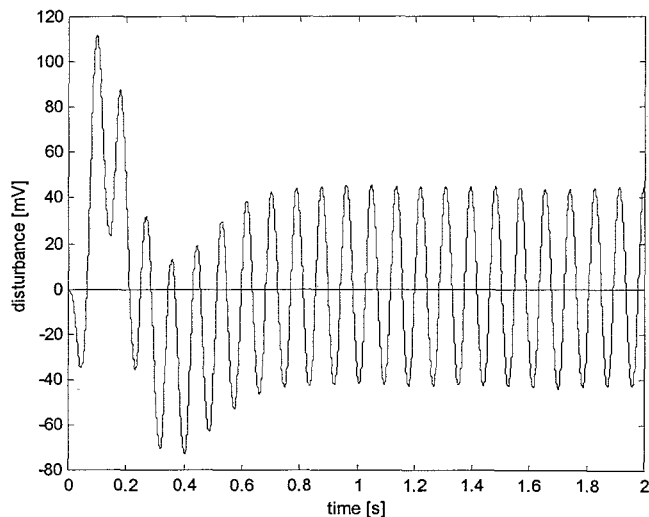

Figure 4.1: radial error signal

Figure 4.2: radial disturbance

The oscillations in the first second are caused by the transient response of the filter. The error specifications as stated in chapter 2 are almost met. The disturbance shows an amplitude around 45 [mV] while the maximum error is 0.05 [mV]. This is a factor 900 compared to the specified factor of 1000. The translation

from [mV] to [μm] is unknown, but this is not relevant here. Assuming that the CD is manufactured with the right specifications the only thing of importance is the magnitude of the error compared to that of the disturbance.

To ensure that the simulator makes use of the true error signal the filter is omitted in the simulations. Now the resulting disturbance d contains the radial disturbance caused by the eccentricity of the disc as well as the noise in the signal. If no algorithm is used to cancel the disturbance the simulator returns the exact same error at "RES 2" as is injected into the system at "RES 1". The setup for the simulations is shown in figure 4.3.
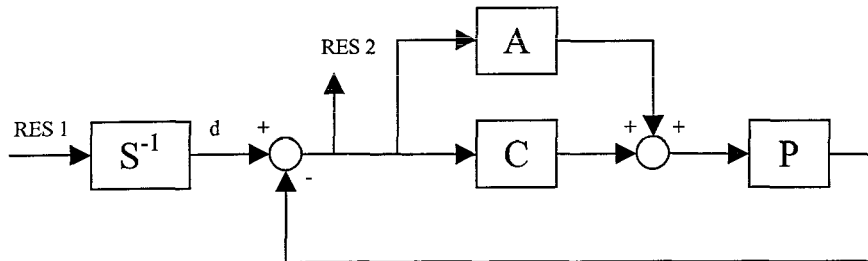

Figure 4.3: Simulation setup

This results in the simple presentation shown in figure 4.4, with S = 1/(1 + CP). Again this is only the case when no algorithm (A) is used.
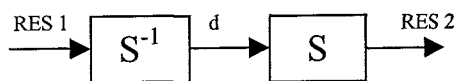

Figure 4.4: Simple representation

The simulation results for the error are shown in figure 4.5. The plot range is set from 1.8 to 2 seconds. The resulting error for the three algorithms is a factor 2.5 smaller compared to the original error signal (for the notch filter this factor is 5). The original reductionfactor of 900 is now increased to 2250 (4500 for the notch).
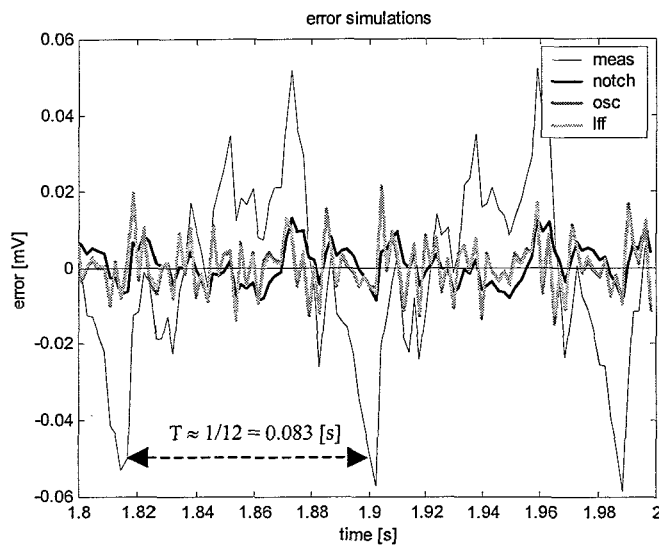

Figure 4.5: Radial error simulations

As was already stated in chapter 2 the error for the oscillator and the learning feedforward are equivalent. The resulting error with the notch filter is somewhat smaller (see figure 4.6). Looking at the power spectra

11

in figure 4.7 it can be seen that the notch filter does not cancel the rotational frequency as good as the oscillator and the LFF, however for higher frequencies the notch filter appears to be better.
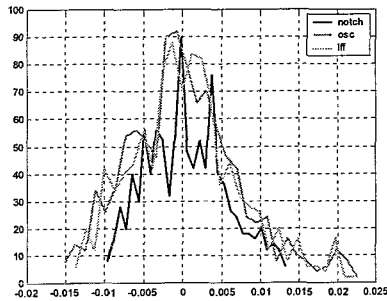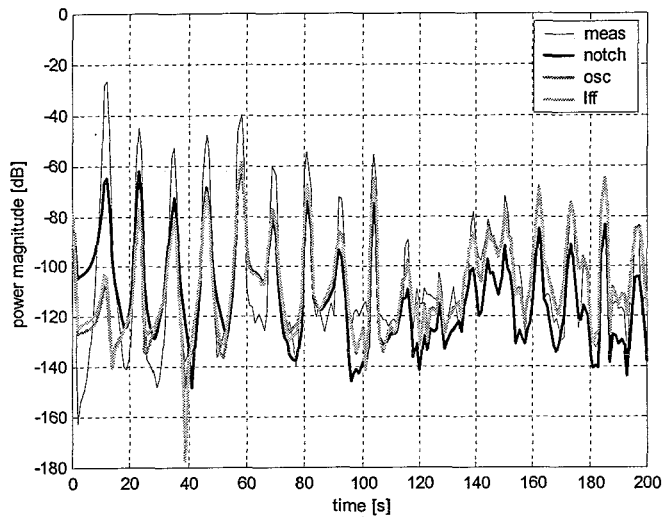

Figure 4.6: Histograms simulated error signals

Figure 4.7: Power spectra error signals

This can be explained by looking at the frequency response function for a notch filter and an oscillator. The bode plots are shown in figure 4.8. For low frequencies the notch and the oscillator behave the same (they both have slope 0), for high frequencies however the oscillator shows a slope of −1 where the notch shows slope 0. So for higher frequencies the notch shows a higher gain compared to the oscillator. This leads to a lower sensitivity at these frequencies (for the sensitivities see figure 2.3). Another effect is an increase in bandwidth. Where the Notch filter has a bandwidth around 600 [Hz], the oscillator has a bandwidth around 350 [Hz] (see figure 4.9 for the bode plots of the open loops). For this reason, the comparison between the algorithms is not a completely fair one.
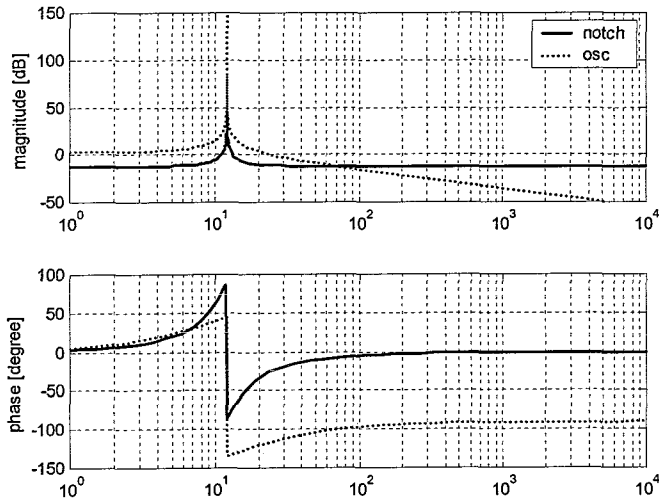
Figure 4.8: Bode plot notch and oscillator
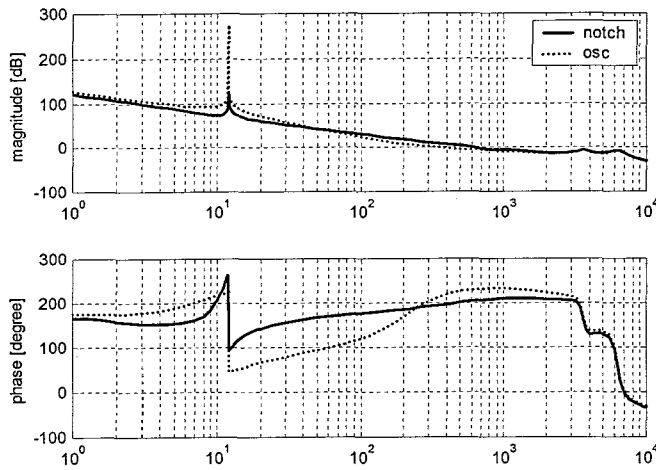
Figure 4.9: Bode plots open loop notch and oscillator, both in combination with the PID

The improvement on the controller can also be seen as an improvement on the track eccentricity of the disc. The simulated error signals for the three algorithms can then be seen as error signals measured on "improved" discs. Filtering the error signals and using the inverse sensitivity of the system, without an algorithm, results in the disturbance signals belonging to these "improved" discs. Figure 4.10 shows these disturbance signals.

disturbance simulations

Figure 4.10: Simulated radial disturbance

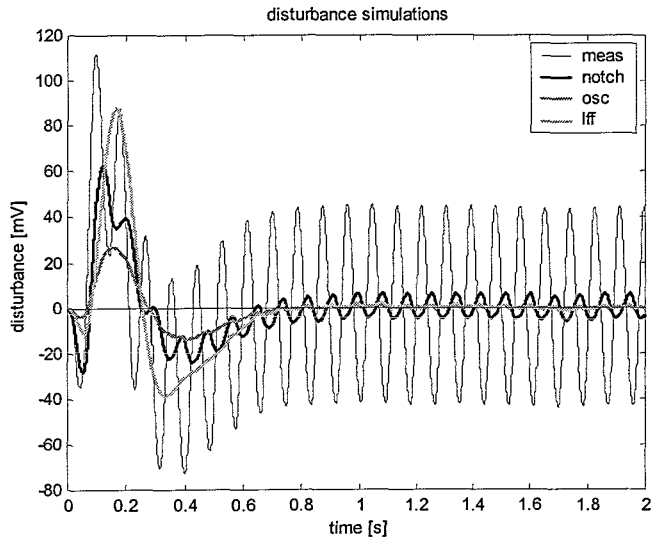Zooming in on the last second, it can be seen that the oscillator and the learning feedforward cancel the disturbance almost completely (from 45 to 2 [mV] meaning a factor 22.5), whereas the notch filter still shows some oscillation (from 45 to 6 [mV] meaning a factor 7.5). So although the notch filter does not cancel the disturbance as good as the oscillator and the feedforward, it does have the smallest radial error (see figures 4.5 and 4.6) thanks to the lower sensitivity at higher frequencies (about 9 [dB] lower, see figure 2.3).
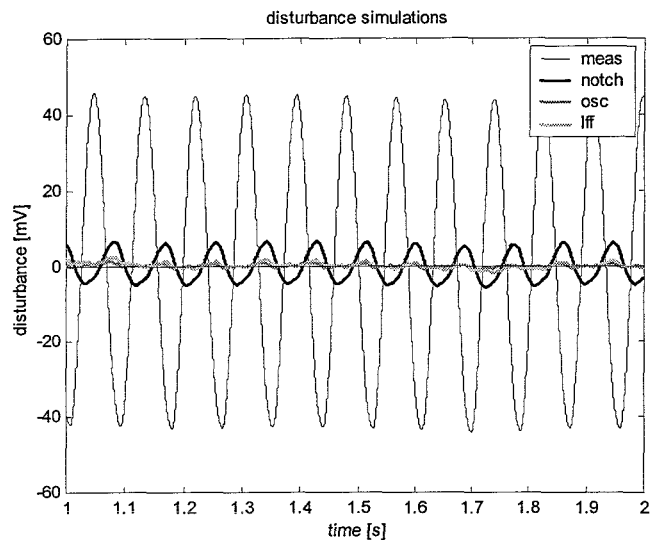
disturbance simulations

Figure 4.11: Simulated radial disturbance, 1-2 sec

4.1 Influence frequency error.

In normal CD-players the rotation frequency varies over the position of the OPU on the disc. For audio CD-players for example the rotation frequency varies from 4 to 8 [Hz] from the outer to the inner track. As was already mentioned in chapter 2, the error signal is a combination of sines and cosines at the rotational frequency and its harmonics. Designing the algorithm with a fixed frequency will result in an error between this frequency and the rotation frequency.

To see what influence this error has on the error- and disturbance signals the three algorithms are designed with three frequencies (10, 12 and 14 [Hz]). Every design is simulated with the measured error signal at 12 [Hz] (see figure 4.1). Figure 4.12 shows the resulting errorsignal.

14
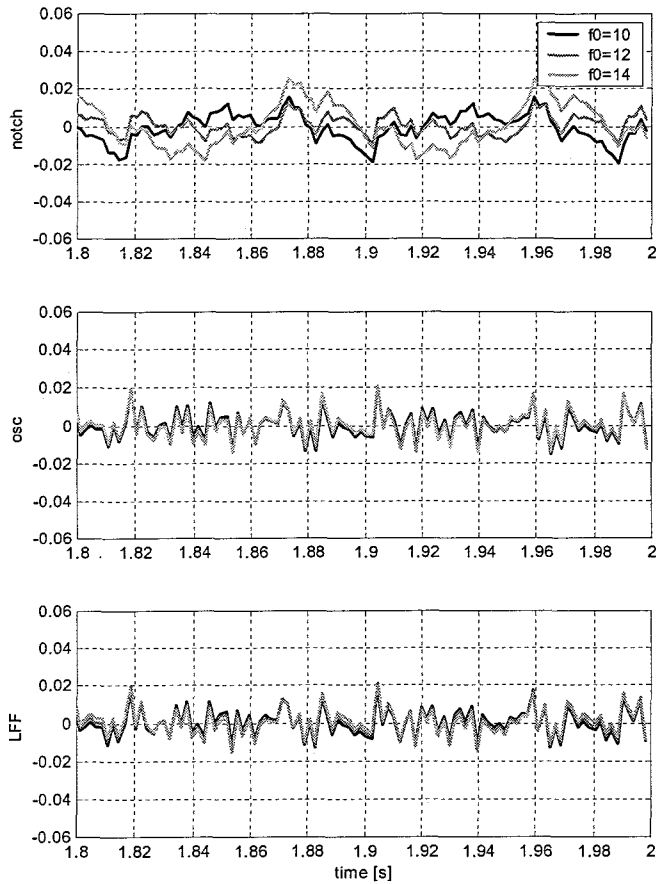
Figure 4.12: Resulting errorsignal for varying frequency

Whereas the error signal does not change significantly for the oscillator and the feedforward, it does for the notch filter. Where the notch shows the smallest error when the right frequency is used, it appears to have the largest error when the frequency is wrong. See figure 4.15 for a histogram of the error for $f_0 = 14$ [Hz].
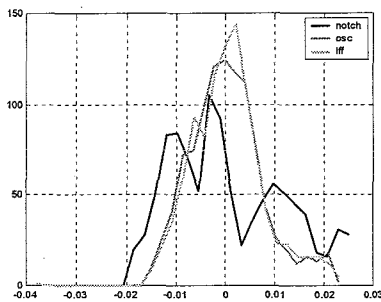

Figure 4.13: Histogram for f_0 =14 [Hz]

When the algorithm is designed at the right frequency the notch filter shows the smallest error and thus the best result. However when the used frequency is wrong, the performance of the notch filter degrades considerably, resulting in the largest error. The oscillator and the feedforward give good results over the whole frequency range (in this case 10-14 [Hz]), and are therefore preferred above the notch filter. Figures 4.14 and 4.15 show the sensitivities for the situations where the notch filter and the oscillator are designed at 10, 12 and 14 [Hz]. The notch filter, designed at 10 [Hz], shows a sensitivity at 12 [Hz] that is about 9 [dB] lower than with the PID. When it is designed at 14 [Hz] the sensitivity is about 6 [dB] lower. The oscillator shows a sensitivity that is 26 [dB] lower than with the PID for both cases.
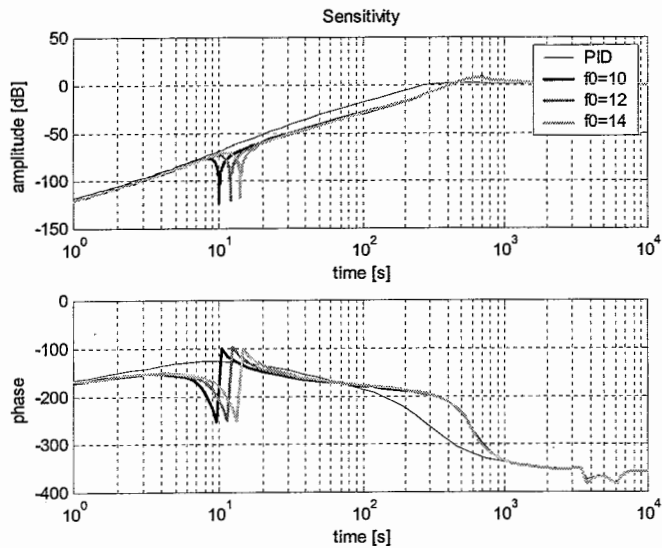

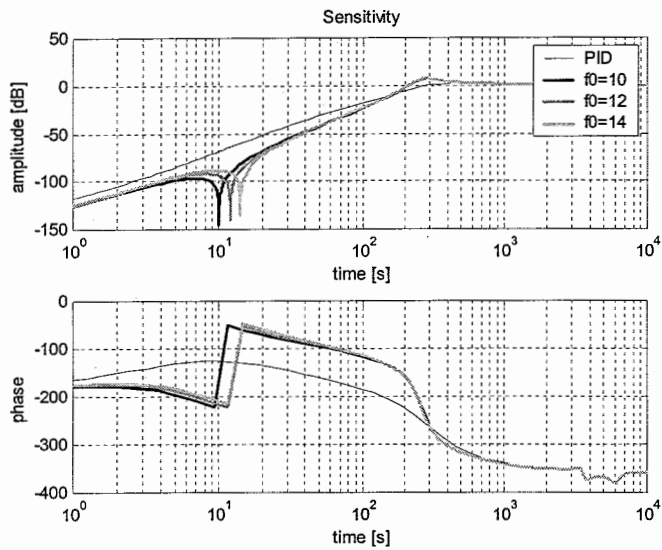Figure 4.14: Sensitivity notch filter, $f_0 = 10, 12, 14$ [Hz]

Figure 4.15: Sensitivity oscillator, $f_0 = 10, 12, 14$ [Hz]

16

5 Measurement results

The simulations in the previous chapter showed promising results. Now it is time to validate these results. The internal controller of the CD player is bypassed with the designed controllers using a Dspace system (sample frequency = 40 [kHz]). The error is measured using the same settings as in the previous chapter (see appendix A).
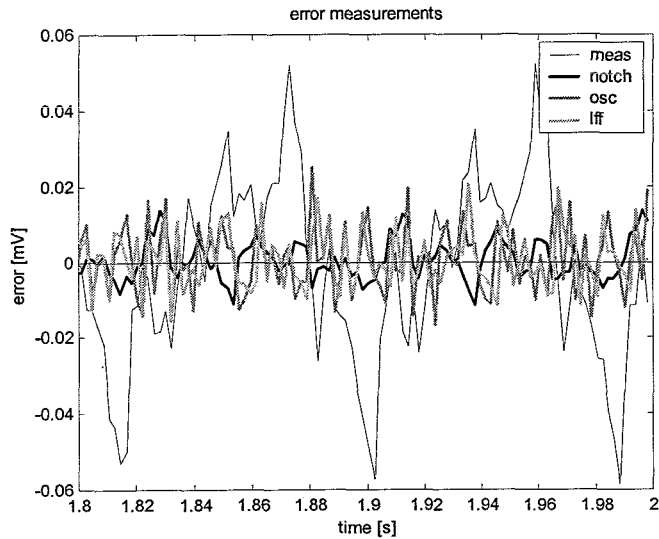
Figure 5.1: Radial error measurements

The measured error signals show great resemblance with the simulated error signals, they are somewhat larger however (compare figure 5.2 with 4.6). The results obtained with the oscillator are indeed equivalent to those obtained with the feedforward and the notch filter shows the smallest error. The power spectra for the error signals are shown in figure 5.3.
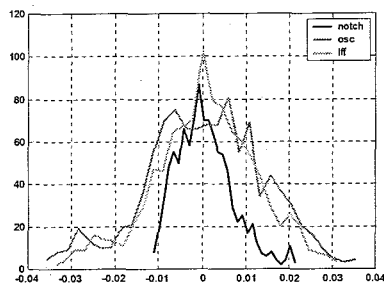
Figure 5.2: Histograms measured error signals
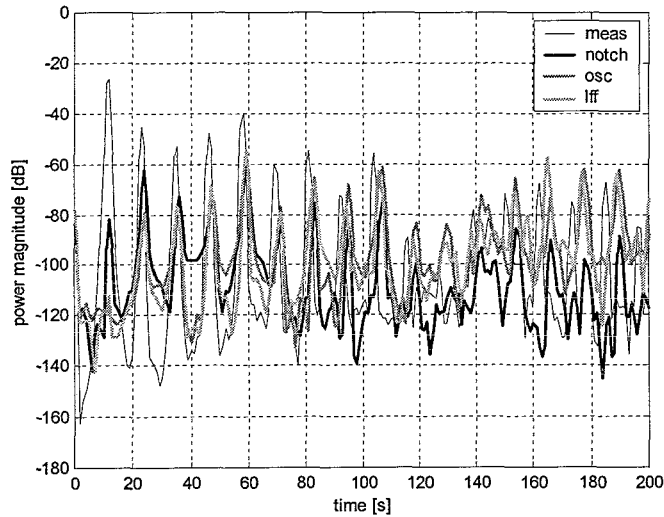
Figure 5.3: Power spectra error signals

In figure 5.4 the simulated power spectra from the previous chapter and the measured ones are compared. The notch filter appears to cancel the rotation frequency better compared to the simulations. The oscillator and the feedforward however still show better cancellation. The fact that the error measured with the notch filter is smaller than with the oscillator or the feedforward is caused by the lower sensitivity at higher frequencies, as was already stated in the previous chapter.

Figure 5.4: Power spectra error signals, 0-50 [Hz]

Filtering the measured error signals and using the inverse sensitivity, as was done in the previous chapter with the simulated error signals, results in the "new" disturbances.

18
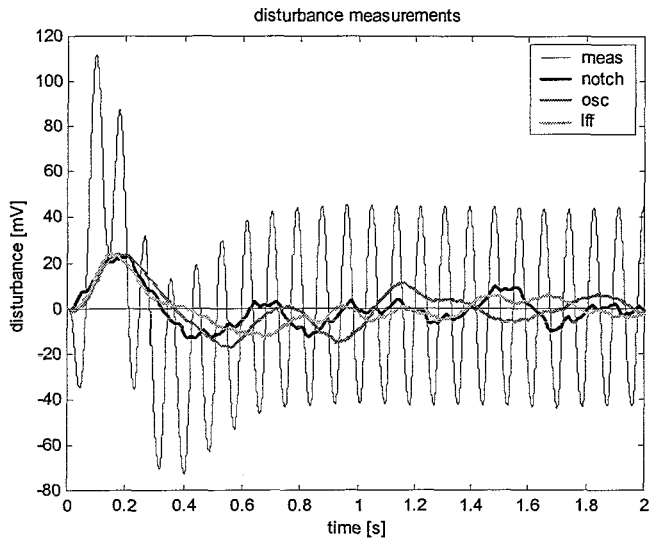
Figure 5.5: "Measured" radial disturbance

Zooming in on the last second, it can be seen that there is not much difference between the three algorithms. In the simulations the oscillator and the LFF cancelled the disturbance with a factor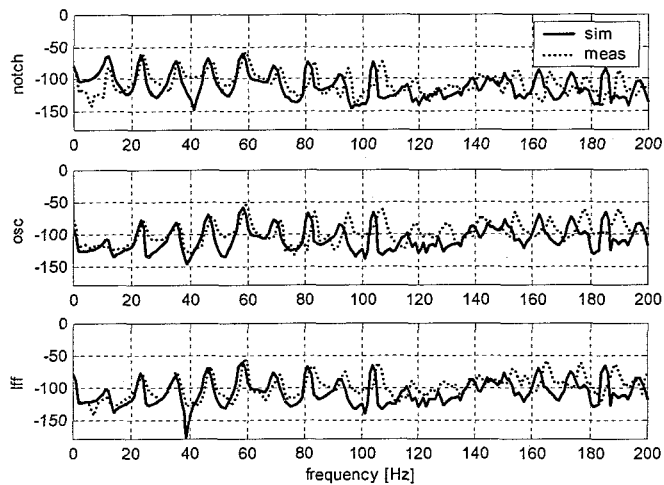 22.5 and the notch filter with a factor 7.5, whereas in the measurements the algorithms cancel the disturbance with a factor 4.5. Although the simulated error signals show great resemblance with the measured error signals, there is some difference in the calculated disturbance signals.
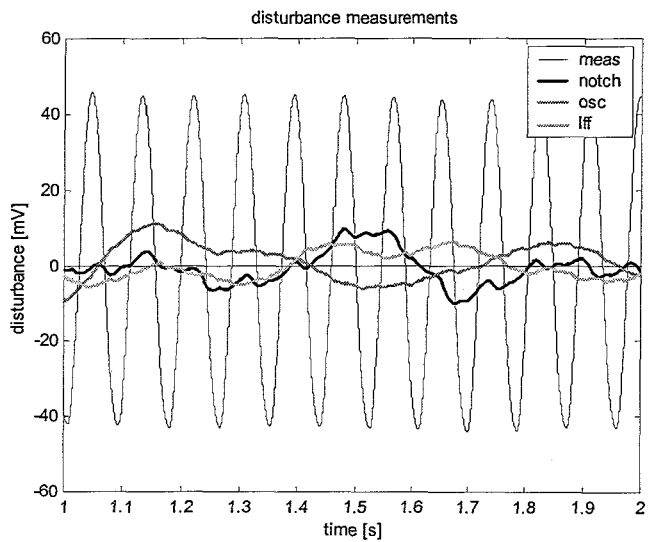
Figure 5.6: "Measured" radial disturbance, 1-2 sec

The main reason for the difference between the simulated and the "measured" disturbance signals is that the controller, after implementing in Dspace, is different from the one used in SimuLink. Figure 5.7 shows the bode plot for the controller with the notch filter in SimuLink and after implementation in Dspace. Other reasons might be unmodeled dynamics and discretisation effects other than the one mentioned above.
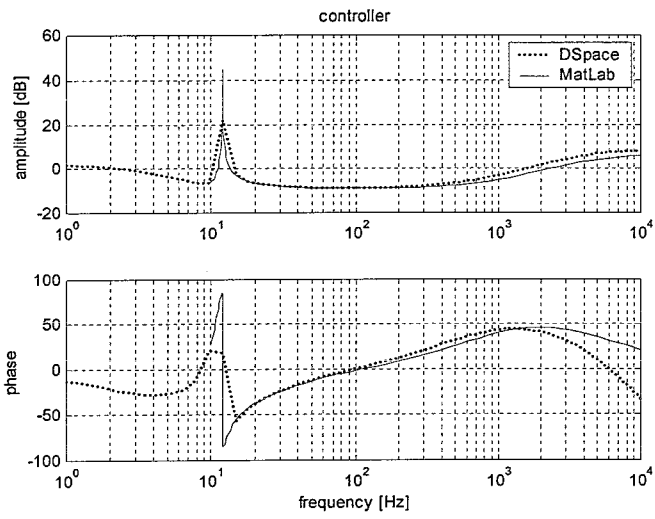
Figure 5.7: Bode plot PID + notch filter

6 Conclusions and Recommendations

The main goal of this report was to see if the Learning Feedforward cancels the periodic disturbance in CD applications better than standard techniques like a notch filter and an oscillator. To this extent the above mentioned algorithms where used in simulations and measurements on a CDM9 player.

The following conclusions can be drawn:
- The Learning Feedforward is equivalent to the internal model principle of the oscillator.
- The notch filter has a higher bandwidth and a lower sensitivity at higher frequencies compared to the oscillator and the feedforward (parallel configuration).
- The notch filter appears to have the best performance when the frequency used in the design of the algorithm is correct.
- When the frequency is incorrect, the performance of the notch filter degrades significantly, whereas the performance of the oscillator and the feedforward remains almost unchanged.

Recommendations:
- The advantage of a feedforward on an oscillator is the fact that a pure feedforward does not influence stability. The learning part of the feedforward however does. After learning the necessary feedback can be turned off, after which the bandwidth can be increased. Further research has to be done to investigate the improvement of the feedforward on the oscillator.
- A way to counteract the influence of the rotation frequency is estimating this frequency. In the case of the learning feedforward adding an extra adaptive law could do the trick. For the notch filter and the oscillator this is a somewhat harder task, but it might be worthwhile to investigate. For the present laboratory setup this is not necessary, since it rotates at a constant frequency.
- To see what the discretesation effects are, the algorithms can be discretised for better comparison between simulations and measurements.
- A way to reach a pure feedforward is to put the eccentricity data on the disc. This information can then be used to cancel the disturbance.
- For better cancellation of the disturbance a repetitive runout algorithm can be used to cancel the rotation frequencies as well as its harmonics.

Bibliography

[1]   Y. Zhou, M. Steinbuch, G. Leenknegt, "Tracking learning feedforward control for high speed CD-rom", it Proc. 1st IFAC conference on Mechatronic Systems, 18-20 September 2000, Darmstadt, pp 961-966

[2]   M. Bodson, A. Sacks, P Khosla, "Harmonic generation in adaptive feedforward cancellation schemes", IEEE trans. on automatic control, vol 39, nr 9 sept 94

[3]   J. Janssens, "Characterization of optical discs", DCT 2001-14, Eindhoven university of technology
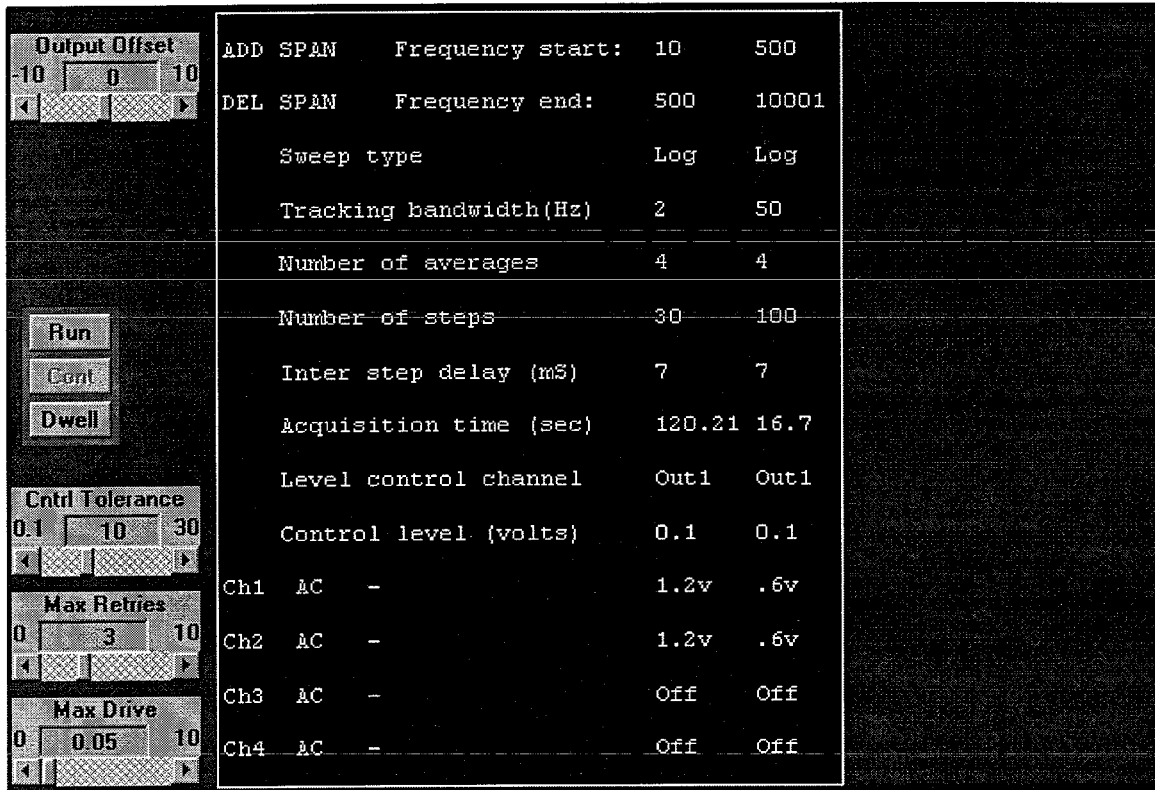
Appendix A: Measurement settings

```
Output Offset          ADD  SPAN      Frequency start:   10      500
-10     0      10
◄▐▒▒▒▒▐░░░░▐  ►        DEL  SPAN      Frequency end:     500     10001

                            Sweep type                   Log     Log

                            Tracking bandwidth(Hz)       2       50

  Run                       Number of averages           4       4

  Cont                      Number of steps              30      100

  Dwell                     Inter step delay (mS)        7       7

                            Acquisition time (sec)       120.21  16.7

Cntrl Tolerance             Level control channel        Out1    Out1
0.1     10     30
◄▐▒▒▒▒▒▐░░░▐  ►            Control level (volts)        0.1     0.1

                       Ch1  AC    -                       1.2v    .6v
Max Retries
0       3      10     Ch2  AC    -                       1.2v    .6v
◄▐▒▒▒▐░░░░░▐  ►
                       Ch3  AC    -                       Off     Off
Max Drive
0      0.05    10     Ch4  AC    -                       Off     Off
◄▐▒▒▒▐░░░░░▐  ►
```

Figure A.0.1: Measurement settings VSS: sensitivity measurements (chapter 2)

```
Ch1  ▼   On        BW=200Hz   ▼
0.31V ▼  AC  ▼     AA Filters On
                   Record Length
                   64    1024   8192
                   ◄▐░░░░░░░░░░▐  ►
  Channel Label      Zoom Off
    Channel 1

EU Off  1    0dB    dF=0.500Hz

Add     ▼   ☐ Zp  Off [Free Run] ▼
  Stop at Count
   1     50   1000
◄▐░░░░░░░░░░░░▐  ►
Ovld Rej    ▼
50% Overlap ▼
Hanning     ▼
```
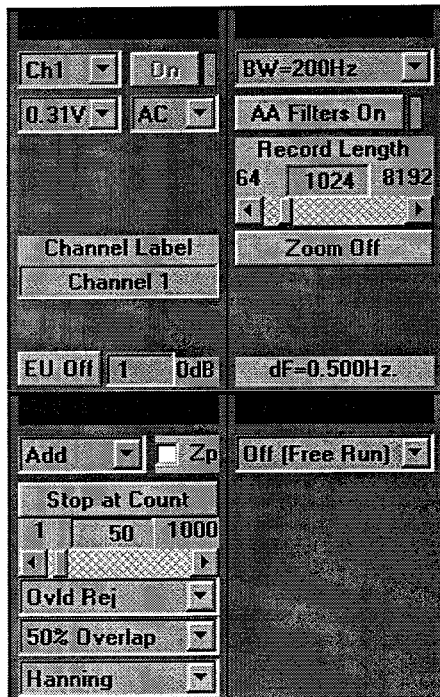
Figure A.0.2: Measurement settings VNA: error measurements (chapter 4 & 5)

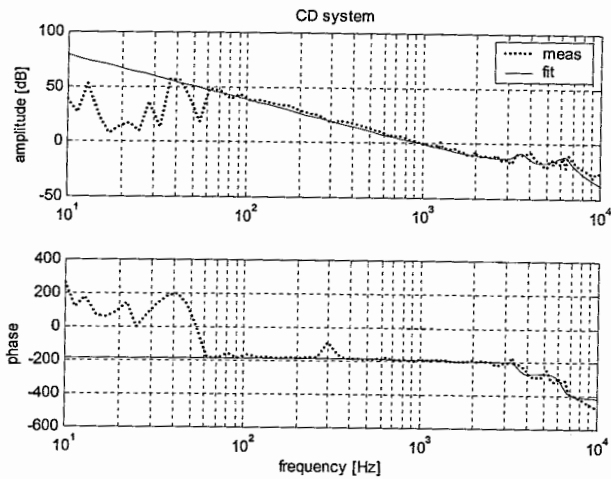# Appendix B: Plant for varying OPU position

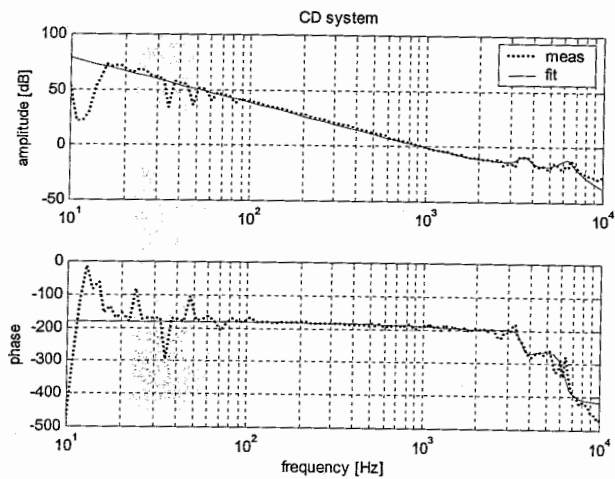Figure B.0.1: Results for the inner track of the disc
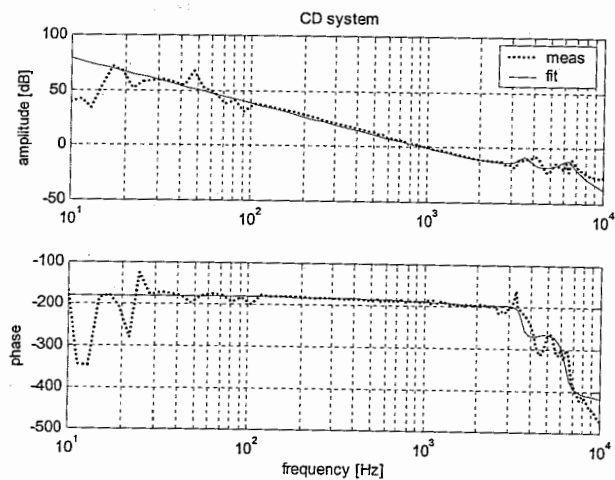

Figure B.0.2: Results for the middle of the disc

Figure B.0.3: Results for the outer track of the disc